Self-consistent optical constants of SiC thin films

Juan I. Larruquert,* Antonio P. Pérez-Marín, Sergio García-Cortés, Luis Rodríguez-de Marcos, José A. Aznárez, and José A. Méndez

GOLD—Instituto de Óptica–Consejo Superior de Investigaciones Científicas, Serrano 144, 28006 Madrid, Spain
*Corresponding author: larruquert@io.cfmac.csic.es

The optical constants of ion-beam-sputtered SiC films have been measured by ellipsometry in the 190 to 950 nm range. The set of data has been extended both toward shorter and longer wavelengths with data in the literature, along with inter- and extrapolations, in order to obtain a self-consistent set of data by means of Kramers–Krönig analysis. All data correspond to films that were deposited by sputtering on nonheated substrates, and hence they are expected to be amorphous. A bandgap of 1.9 eV for the films was fitted from the obtained optical constants. A good global accuracy of the data was estimated through the use of various sum rules. The consistent dataset includes the visible to the extreme ultraviolet (EUV); this large spectrum of characterization will enable the design of multilayer coatings that combine a high reflectance in parts of the EUV with desired performance at a secondary range, such as the visible. To our knowledge, this paper provides the first compilation of the optical constants of amorphous SiC films.   © 2011 Optical Society of America

OCIS codes: 120.4530, 160.6000, 310.6860, 260.7200, 230.4170.

1. INTRODUCTION

SiC is a material with an increasing number of applications, due to a combination of several properties, such as a wide-bandgap semiconductor, high radiation resistance, stability at high temperatures, and high thermal conductivity. As an optical material, it has been used for its moderately high reflectance in the extreme ultraviolet [(EUV)—here it will refer to wavelengths shorter than 190 nm], mainly in the ~50 to 180 nm range. The largest EUV reflectance of SiC is obtained both with single crystals and with films prepared by chemical vapor deposition (CVD) [1,2]. A somewhat lower EUV reflectance is obtained for SiC deposited by sputtering [3,4], although the latter method has the advantage over CVD that it does not require hot-substrate deposition and the layer grows smoothly. EUV multilayers have also been developed in which sputtered–deposited SiC films are incorporated to the multilayer both as a constituent [5–9] as well as a barrier layer or capping layer for high-reflectance coatings at wavelengths longer than the Si $L_{2,3}$ edge at ~12.4 nm.

Even though there is a large number of papers reporting optical constants (often only the absorption coefficient) of SiC films in the visible and close ranges and in the reststrahlen region, we found almost no papers in which SiC is investigated as an optical material for coatings longward of ~200 nm, with a few exceptions [5,7–10]. The material itself does not have attractive optical constants for optics in the visible and close ranges, because it has a relatively large absorption and yet not a high enough reflectance. However, there are applications for EUV coatings that require a certain performance at a secondary range, such as the visible (for instance a rejection of the visible would be desirable for EUV coatings when solar-blind detectors are not available), which makes important the availability of a set of optical constants in a broad spectral range.

For crystalline SiC, Choyke and Palik [11] reviewed the optical-constant data that were available for the 6H SiC

(hexagonal crystal) polytype. However, in various ranges of the spectrum, the optical constants of crystalline and amorphous SiC are expected to be rather different [12], which makes necessary the compilation of a specific set of data for amorphous SiC. The purpose of this paper is to provide optical constants of amorphous SiC films prepared by sputtering on nonheated substrates in a broad spectral range. This paper provides new data measured by ellipsometry in the 190 to 950 nm range and extends this range with literature data and inter- and extrapolations both at shorter and at longer wavelengths. Section 2 describes the equipment used for sample deposition and characterization. Section 3 displays the obtained optical constants n, k of SiC and their extension both to the EUV and to wavelengths longer than the reststrahlen band. Kramers–Krönig (KK) analysis was used to obtain a self-consistent set of data. Sum rules are used to estimate the global accuracy of the data.

2. EXPERIMENTAL TECHNIQUES

SiC samples were prepared by ion-beam sputtering (IBS), i.e., by impinging energetic ions at 25° on a target placed facing the substrate. A 96.5 mm diameter, 99.9995% purity CVD SiC target was used. The target was placed in a rotatable target holder that hosts up to four targets that are cooled down with water. Ions were produced by means of a 3 cm hollow cathode ion gun working with a hollow cathode neutralizer; this gun and neutralizer contain no filament, which minimizes contamination. Typical deposition conditions were: ion energy of 1, 200 eV and a total ion current of 45 mA. Ar was used as a process gas. Thin films were deposited at a rate of ~0.09 nm/s. The film thickness was measured during deposition with a quartz crystal monitor. Si wafers were used as substrates for ellipsometry measurements. A witness glass sample was coated at the same time as the Si substrate; the film thickness of the witness sample was measured *a posteriori* through Tolansky interferometry, i.e., through multiple-beam interference fringes in a wedge

between two highly reflective surfaces [13]. The target-to-substrate distance was 15 cm. The substrate was not intentionally heated or cooled. The sputtering deposition system is placed in a ultrahigh-vacuum (UHV) chamber pumped with a cryopump. The base pressure was 7×10^{-8} Pa in the sputtering chamber. During deposition, the chamber reached a total pressure of 6×10^{-2} Pa.

Ellipsometry measurements were performed with a SOPRALAB GES5E spectroscopic ellipsometer. The incidence angle at which measurements were performed was optimized around the Si Brewster angle at the Si bandgap by confining the spectral distribution of $\cos \Delta$ symmetrically around zero in order to maximize accuracy. Measurements were performed on samples immediately after taking them out of the vacuum chamber. Ellipsometry measurements started ~5 min after first contact with the atmosphere, and they lasted roughly 30 min. Exposure to air was made as short as possible before ellipsometry measurements in order to minimize the oxidation of the samples prior to measurements, so that the intrinsic optical constants of SiC could be measured.

3. RESULTS AND DISCUSSION

A. Determination of Optical Constants
Three samples of SiC were prepared, with thicknesses of 29, 32, and 41 nm. Ellipsometry measurements were performed at incidence angles of 72° to 74° in the 190 to 950 nm range, and the optical constants n and k were calculated at each measured wavelength. No model for the optical constants of SiC was assumed in the calculation. Figure 1 displays the ellipsometry parameters $r_p/r_s = \tan(\psi)e^{i\Delta}$ measured at 72° for the 29 nm thick sample and the fit with the derived optical constants. Figure 2 displays the obtained optical constants averaged over the three samples. Error bars represent the standard deviation over the three samples; error bars cannot be individually distinguished, but the curve thickness stands for the error-bar length. The standard deviation, averaged both over the three samples and over the spectrum, amounts 0.020 for n and 0.016 for k. Likewise, we obtain a relative deviation, normalized to n or k, of 0.006 for n and 0.05 for k; the relative deviation for k increases with wavelength due to the decrease of k. In the calculations, surface roughness was neglected.

Literature data were searched to compare with our data, which are displayed in Fig. 3. Data have been published for SiC films deposited by techniques such as CVD or sputtering,
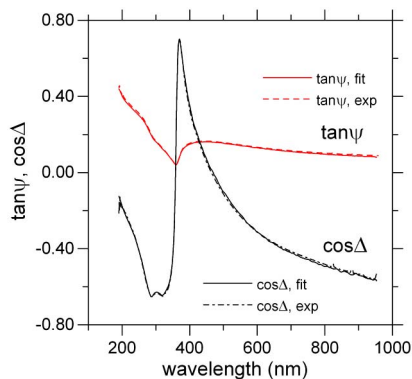
Fig. 1.   (Color online) Ellipsometry parameters $\tan \psi$ and $\cos \Delta$, both experimental and fitted, as a function of wavelength.
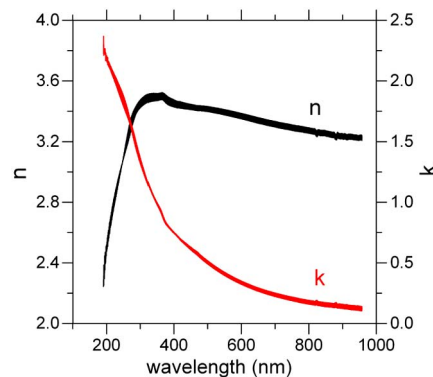
Fig. 2.   (Color online) Optical constants n and k obtained from ellipsometry measurements as a function of wavelength. The curve thickness stands for the error-bar length.

on substrates either at room or at hot temperatures, for both as-deposited or annealed samples; furthermore, techniques like CVD or sputtering may involve the addition of species into the film, such as H or F; additionally, there are data for crystal samples that have been amorphized by impinging energetic ions. All these multiple variables result in a wide variety of optical-constant data that will not agree with each other. Here we have restricted our comparison to data obtained on
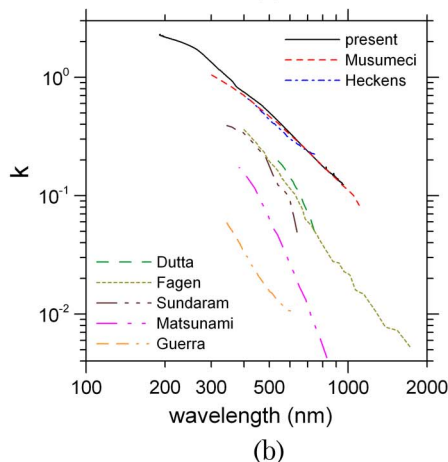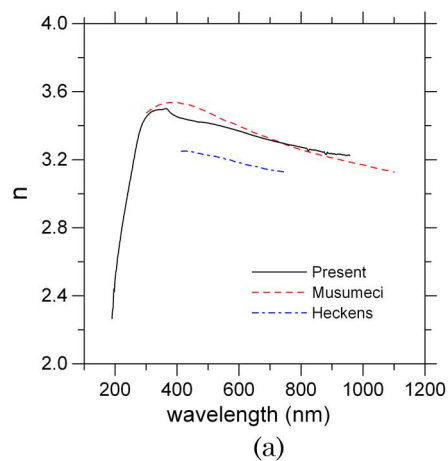
Fig. 3.   (Color online) (a) Obtained optical constants n and (b) the logarithm of k versus energy (a) and its logarithm (b) compared with the literature data of Fagen [14], Matsunami *et al.* [15], Dutta *et al.* [16], Heckens and Woollam [17], Sundaram *et al.* [18], Guerra *et al.* [19], and Musumeci *et al.* [20].

samples deposited by sputtering on room-temperature substrates, or at least on substrates not hotter than 370 K, because these are the conditions that we expect for the use of SiC films in multilayers for optics. A hotter substrate is expected to result in a less-absorbing layer, which would be mostly beneficial for optical coatings; however, for many applications heating the substrate is not feasible, due to possible material limit, either the substrate or any multilayer constituent, and to the possible growth of stress. Regarding various sputtering techniques, we consider that IBS and magnetron sputtering are similar techniques that may provide films with close optical constants. In Fig. 3 we compare our data with data from the literature selected as mentioned above; data include Fagen [14], Matsunami *et al.* [15], Dutta *et al.* [16], Heckens and Woollam [17], Sundaram *et al.* [18], and Guerra *et al.* [19]; most data include only *k*. There is a large dispersion of *k* data. Only the Heckens *k* data match the present one; the match of the Heckens data in *n* is not as good as in *k*, but the differences are not very large. In fact, film thicknesses in Heckens and Woollam's research, even though a factor of roughly three larger than our films, are the closest among the aforementioned papers, whereas all others involve much larger film thicknesses ranging between 350 nm and 16 μm.

Additionally, we have represented the data of Musumeci *et al.* [20] for as-implanted samples, even though they correspond to 6H-SiC crystals that were amorphized with 200 keV Kr ions; we display these data for comparison, even though sample preparation is very different, because they give the best match to our data, both *n* and *k*. The wide differences in optical constants over the literature may be due to differences in film thickness and in the film growth or aging, and the literature does not display extensive information on this. Regarding our samples, they were deposited in UHV with the use of clean pumping, and atmospheric exposure was minimized (within ∼35 min exposure), which suggests that in our samples contamination may have been minimized. The presented *n*, *k* data are the first to extend visible measurements down to the beginning of the EUV at 190 nm.

In order to generate a set of optical constants that includes at least from the EUV range (where SiC has a large reflectance) to the near infrared, so that multilayer coatings can be designed for such a broad range, we extended the present range with data from the literature. We gathered *k* data over the whole spectrum, and then we generated *n* with KK analysis; finally, we compared the latter *n* data with our original data measured by ellipsometry. In the extension to the EUV range, we used the *k* data of Fernández-Perea *et al.* [21] for IBS SiC films in the 58.4 to 149.2 nm range; those measurements were performed *in situ* and hence they are expected to be somewhat more accurate than other data obtained after some contact to atmosphere [12]. In this range, it is important to use *in situ* data, because a very thin oxide film that grows on SiC upon contact with the atmosphere affects in a measurable way an optical function such as reflectance, and hence the optical constants calculated from it; this effect is expected to be mostly negligible at longer wavelengths because the thin oxide film will absorb less there. There was a gap between the present data and the Fernández-Perea data, which was filled with a smooth connection; for this connection, Ref. [12] was used as a help. At even shorter wavelengths, we used the data of Kortright and Windt [4], down to 41 nm (30 eV); this shorter

wavelength range will be expressed in electron volts. Above 30 eV, we used the data of Henke *et al.* [22], who obtained a semiempirical set of data in the 30 to 10,000 eV range (later extended to 30,000 eV [23]). The density of SiC amorphous films adopted here was 2.98 g/cm³, and it was taken from Soufli *et al.* [24], who measured it for DC magnetron-sputtered SiC films that were deposited on a room-temperature substrate. The Henke data were downloaded from the Web site of The Center for X-Ray Optics (CXRO) at Lawrence Berkeley National Laboratory [25]. These data were extrapolated to still higher energies with a power function.

The extension to longer wavelengths was more difficult, because we found no usable data in the literature in the range of ∼1.1 to 8 μm. As an amorphous semiconductor, SiC film optical-constant data could be fitted in principle with a Tauc–Lorentz model [26]. However, that model assumes no absorption in the range below the bandgap of the material, which for SiC is expected to be in the ∼1.6 to 2.0 eV range [14,15,18] (Ref. [15] was obtained for samples deposited at 373 K). But of course material absorption is not zero at energies just below the bandgap, so that the Tauc–Lorentz model is not useful to describe this range. In view of the above, we decided to use the optical constants of a close material; amorphous Si was found as the closest amorphous semiconductor material for which optical constants were available. The *k* of amorphous Si was taken from Pierce and Spicer [27] in the spectral range longer than 950 nm. In order to smoothly connect to our data, we multiplied the Pierce and Spicer *k* data by a factor of 1.96. At a still longer wavelength, SiC presents the absorption corresponding to the reststrahlen band, which is much smoother for amorphous than for crystalline SiC. There are various papers with data on the reststrahlen band for SiC prepared by different methods. We selected the data published by Fagen [14]. We fitted a Lorentz oscillator to the plotted absorption coefficient and used this oscillator to extrapolate the data both to longer wavelengths and to connect with the normalized data of Pierce and Spicer at shorter wavelengths.

With this set of *k* in the whole spectrum we could calculate the refractive index *n* of SiC in the whole spectrum using KK dispersion relations:

$$n(E) - 1 = \frac{2}{\pi} P \int_0^\infty \frac{E' k(E')}{E'^2 - E^2} \mathrm{d}E', \tag{1}$$

where *P* stands for the Cauchy principal value and *E* stands for photon energy. Because we also had measurements of *n* in the 190 to 950 nm range, we could check the similarity of both datasets in this range. *n* data obtained through KK analysis were larger than data obtained by ellipsometry; the difference averaged ∼3.2%. From our ellipsometry measurements, so far only *k* data have been used. In order to involve also ellipsometry *n* data in the calculation of self-consistent optical-constant data of SiC, we constructed a new set of *n* data in the following way. In the spectral range of ellipsometry measurements, we averaged *n* data between ellipsometry data and the data obtained through KK analysis. At longer wavelengths, *n* data obtained through KK analysis were normalized to connect with the above averaged dataset in the 190 to 950 nm range. At shorter wavelengths, the original *n* data obtained through KK analysis were kept with a smooth connection. This new and complete set of *n* data was used in an inverse KK analysis:

$$k(E) = -\frac{2E}{\pi} P \int_0^\infty \frac{[n(E') - 1]}{E'^2 - E^2} dE', \qquad (2)$$

so that a new set of k data was obtained. This set was now compared to k data obtained by ellipsometry, and the new data were ~1% lower than ellipsometry measurements on average, which was considered an acceptable difference for the new set to describe film optical properties. This consistent set of n, k data was taken as the final result, and it is plotted in Fig. 4 [28] in the spectral range including from the reststrahlen band to the Si L$_{2,3}$ edge.

For crystalline semiconductors, the bandgap is a well-defined parameter, which corresponds to energies of forbidden transitions between the valence and the conduction bands. For amorphous semiconductors, Tauc *et al.* [29,30] interpreted the presence of some kind of bandgap as representative of optical transitions without momentum conservation between extended states in the valence and conduction bands under the assumption of parabolic bands and constant matrix elements [31]. The bandgap is calculated as a fitting parameter of ε_2 (imaginary part of the dielectric constant) or the absorption coefficient [32]. Figure 5 displays a Tauc plot obtained with the present optical constants by the fitting equation:

$$\sqrt{\alpha E} \propto (E - E_G), \qquad (3)$$

where α is the absorption coefficient and E_G is the fitted bandgap energy [32]. From Fig. 5 we obtain $E_G = 1.9$ eV by the abscissa intercept of the linear extrapolation. In fact, our curve
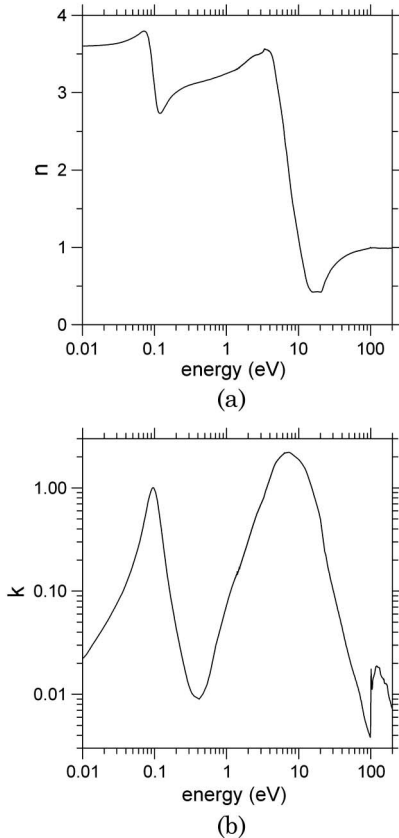

Fig. 4. (a) Self-consistent set of SiC optical constants n and (b) the logarithm of k versus the logarithm of photon energy in a spectral range including from the reststrahlen band to the Si L$_{2,3}$ edge.
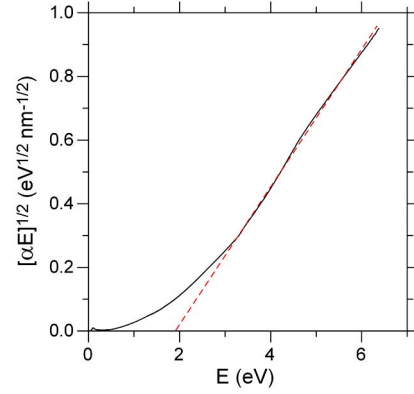

Fig. 5. (Color online) Tauc plot for amorphous SiC; the bandgap is obtained as the abscissa intercept of the linear extrapolation of $\sqrt{\alpha E}$.

approaches very good linearity between ~3.3 and 6.3 eV. The linearity is less perfect when the above function is replaced with the function originally proposed by Tauc [29,30], i.e., $\sqrt{\varepsilon_2 E^2}$, with $\varepsilon_2 = 2nk$ (imaginary part of the dielectric constant), because n is not constant in this range; the latter can be fitted only in the reduced 3.3 to 4.5 eV range and a bandgap of 1.9 eV is also obtained. A bandgap value of 2.0 eV was obtained by Sundaram *et al.* [18] for nonannealed samples, although using their rather different k data compared to the present data. On the other hand, Fagen [14] obtained a bandgap of 1.6 eV (for sample thickness between 0.6 and 16.5 μm, i.e., much thicker than our samples) and Dutta *et al.* [16] obtained a value of only 1.35 eV for an unfluorinated sample. We suggest that the cleanliness of our deposition chamber and the fast measurements immediately after sample exposure to the atmosphere make our optical constants more accurate to calculate the bandgap.

B. Consistency of Optical Constants

The f-sum rule relates the number density of the electrons to k or to other functions; it provides a guide to evaluate the global accuracy of k data. It is useful to define the effective number of electrons per atom $n_{\text{eff}}(E)$ contributing to k up to given energy E:

$$n_{\text{eff}}(E) = \frac{4\varepsilon_0 m}{\pi N_{\text{mol}} e^2 \hbar^2} \int_0^E E' k(E') dE', \qquad (4)$$

where N_{mol} is the molecular density, e is the electron charge, ε_0 is the permittivity of vacuum, m is the electron mass, and $\hbar$ is the reduced Planck constant [33]. The f-sum rule expresses that the high-energy limit of n_{eff} must reach the number of electrons of the atom or molecule involved, which is 20 for SiC. When the relativistic correction on scattering factors is taken into account, the high-energy limit of Eq. (4) is slightly modified. The following modified electron number was adopted here [34]: 19.97. The high-energy limit that we obtained using Eq. (4) with the consistent dataset described in the previous subsection was 19.68, which is a mere 1.5% smaller than the theoretical value. As mentioned above, the density of SiC amorphous films to calculate N_{mol} was taken as 2.98 g/cm^3. From the above number of electrons, ~0.45 comes from the spectral range measured by ellipsometry. A larger number of electrons that contribute in this same spectral range is obtained when we replace k in Eq. (4) with ε_2 [35]:

the number of electrons contributing in the ellipsometry range is then ∼1.48; with the latter function, the high-energy limit of n_{eff} differs from the one obtained with Eq. (4) in only 0.004. Looking at these results, we expect that the above small difference in $n_{\text{eff}}(\infty)$ with respect to the predicted number originates over the large spectrum gathered here, and not specifically over the ellipsometry range.

A useful test to evaluate the accuracy of KK analysis is obtained with the inertial sum rule:

$$\int_0^\infty [n(E) - 1] \mathrm{d}E = 0, \tag{5}$$

which expresses that the average of the refractive index throughout the spectrum is unity. The following parameter is defined to evaluate how close to zero the integral of Eq. (5) [36] is

$$\zeta = \frac{\int_0^\infty [n(E) - 1] \mathrm{d}E}{\int_0^\infty |n(E) - 1| \mathrm{d}E}. \tag{6}$$

Shiles *et al.* [33] suggested that a good value of ζ should stand within ± 0.005. An evaluation parameter $\zeta = 2 \times 10^{-4}$ was obtained with the n data calculated in this research. Therefore, the inertial sum rule test is well within the above top value. The main contribution to the integral of Eq. (5) comes from a broad spectral range of ∼0.02 to 5000 eV, which includes the present ellipsometry range but also many data in a broader range, and has a peak contribution at 10.7 eV. As with the f-sum rule, we looked for a specific sum rule that gives more weight to the ellipsometry range. For this, an interesting sum rule is obtained by replacing n with ε_1 (the real part of the dielectric constant; Eq. 37 in Ref. [35]) in Eq. (5); in this case, we must assume a negligible DC material conductivity for the integral to be zero, which seems plausible for amorphous SiC and compatible with the data gathered here. With this sum rule, an evaluation parameter [immediately generalized from Eq. (6)] of 5×10^{-5} was obtained, which is even lower than the one obtained above. The main contribution to the integral comes from a similar range than above, but the peak is now at 6.4 eV, which is very close to the high-energy edge of the present ellipsometry range. This suggests, along with the f-sum rule, a good consistency of the n and k dataset gathered here.

The present self-consistent dataset aims at enabling the design of multilayer coatings based on SiC films with optimized performance in the EUV to near infrared. This task adds to our past efforts to provide similar sets of data on other semiconductors (B [37]) and insulators (SiO [38]), which will be further extended in the near future with more materials.

4. CONCLUSIONS

The optical constants n and k of thin IBS SiC films, which were deposited on room-temperature substrates, have been obtained from ellipsometry measurements in the 190 to 950 nm spectral range. This dataset has been extended to a broad spectrum with the literature data, and inter- and extra-polations. With the use of direct and inverse KK analysis, we have constructed a consistent set of optical constants; this set will enable the design of coatings optimized over a broad spectral range that includes from the EUV, where SiC mirrors have

a large reflectance, to the near infrared. That set is useful for applications for which, in addition to a high reflectance in the EUV, a certain performance is required at a secondary range, such as the visible. A bandgap energy of 1.9 eV was obtained as a fitting parameter involving measurements of the absorption coefficient.

The evaluation of f- and inertial sum rules shows good consistency of the optical constants gathered for SiC.

REFERENCES AND NOTES

1. W. J. Choyke, W. D. Partlow, E. P. Supertzi, F. J. Venskytis, and G. B. Brandt, "Silicon-carbide diffraction grating for the vacuum ultraviolet: feasibility," Appl. Opt. **16**, 2013–2014 (1977).
2. M. M. Kelly, J. B. West, and D. E. Lloyd, "Reflectance of silicon carbide in the vacuum ultraviolet," J. Phys. D **14**, 401–404 (1981).
3. R. A. M. Keski-Kuha, J. F. Osantowski, H. Herzig, J. S. Gum, and A. R. Toft, "Normal incidence reflectance of ion beam deposited SiC films in the EUV," Appl. Opt. **27**, 2815–2816 (1988).
4. J. B. Kortright and D. L. Windt, "Amorphous silicon carbide coatings for EUV optics," Appl. Opt. **27**, 2841–2846 (1988).
5. J. I. Larruquert and R. A. M. Keski-Kuha, "Multilayer coatings with high reflectance in the EUV spectral region from 50 to 121.6 nm," Appl. Opt. **38**, 1231–1236 (1999).
6. J. I. Larruquert and R. A. M. Keski-Kuha, "Sub-quarterwave multilayer coatings with high reflectance in the extreme ultraviolet," Appl. Opt. **41**, 5398–5404 (2002).
7. T. Ejima, A. Yamazaki, T. Banse, K. Saito, Y. Kondo, S. Ichimaru, and H. Takenaka, "Aging and thermal stability of Mg/SiC and Mg/Y$_2$O$_3$ reflection multilayers in the 25–35 nm region," Appl. Opt. **44**, 5446–5453 (2005).
8. R. Soufli, D. L. Windt, J. C. Robinson, E. A. Spiller, F. J. Dollar, A. L. Aquila, E. M. Gullikson, B. Kjornrattanawanich, J. F. Seely, and L. Golub, "Development and testing of EUV multilayer coatings for the Atmospheric Imaging Assembly instrument aboard the Solar Dynamics Observatory," Proc. SPIE **5901**, 59010M (2005).
9. B. Kjornrattanawanich, D. L. Windt, J. F. Seely, and Yu. A. Uspenskii, "SiC/Tb and Si/Tb multilayer coatings for extreme ultraviolet solar imaging," Appl. Opt. **45**, 1765–1772 (2006).
10. U. Schühle, H. Uhlig, W. Curdt, T. Feigl, A. Theissen, and L. Teriaca, "Thin silicon carbide coating of the primary mirror of VUV imaging instruments of solar orbiter," in *The Second Solar Orbiter Workshop*, E. Marsch, K. Tsinganos, R. Marsden, and L. Conroy, eds., ESA SP-641 (ESA Publications Division, 2007), paper P83.
11. W. J. Choyke and E. D. Palik, "Silicon carbide (SiC)," in *Handbook of Optical Constants of Solids*, E. D. Palik, ed. (Academic, 1985), pp. 587–596.
12. J. I. Larruquert and R. A. M. Keski-Kuha, "Reflectance measurements and optical constants in the extreme ultraviolet for thin films of ion-beam-deposited SiC, Mo, Mg$_2$Si, and InSb and of evaporated Cr," Appl. Opt. **39**, 2772–2781 (2000).
13. S. Tolansky, *Multiple-Beam Interferometry of Surfaces and Films* (Oxford Univ. Press, 1948).
14. E. A. Fagen, "Optical and electrical properties of amorphous silicon carbide films," in *Amorphous and Liquid Semiconductors*, J. Stuke and W. Brenig, eds. (Taylor & Francis, 1974), Vol. 1. It contains part of the proceedings of the International Conference on Amorphous and Liquid Semiconductors held at Garmisch-Partenkirchen, Germany, in 1973.
15. H. Matsunami, H. Masahiro, and T. Tanaka, "Structures and physical properties of sputtered amorphous SiC films," J. Electron. Mater. **8**, 249–260 (1979).

16. R. Dutta, P. K. Banerjee, and S. S. Mitra, "Amorphous silicon-carbon-fluorine alloy films," Phys. Rev. B **27**, 5032–5038 (1983).

17. S. Heckens and J. A. Woollam, "*In-situ* ellipsometry on sputtered dielectric and magneto-optic thin films," Thin Solid Films **270**, 65–68 (1995).

18. K. B. Sundaram, Z. Alizadeh, and L. Chow, "The effects of oxidation on the optical properties of amorphous SiC films," Mater. Sci. Eng. B **90**, 47–49 (2002).

19. J. A. Guerra, L. Montañez, O. Erlenbach, G. Galvez, F. De Zela, A. Winnacker, and R. Weingärtner, "Determination of the optical bandgap and disorder energies of thin amorphous SiC and AlN films produced by radio frequency magnetron sputtering," J. Phys. **274**, 012113 (2011).

20. P. Musumeci, R. Reitano, L. Calcagno, F. Roccaforte, A. Makhtari, and M. G. Grimaldi, "Relaxation and crystallization of amorphous silicon carbide probed by optical measurements," Philos. Mag. B **76**, 323–333 (1997).

21. M. Fernández-Perea, J. A. Méndez, José A. Aznárez, and Juan I. Larruquert, "*In situ* reflectance and optical constants of ion-beam-sputtered SiC films in the 58.4 to 149.2 nm region," Appl. Opt. **48**, 4698–4672 (2009).

22. B. L. Henke, P. Lee, T. J. Tanaka, R. L. Shimabukuro, and B. K. Fujikawa, "Low-energy x-ray interaction coefficients: photoabsorption, scattering, and reflection, $E = 100$–2000 eV, $Z = 1$–94," At. Data Nucl. Data Tables **27**, 1–144 (1982).

23. B. L. Henke, E. M. Gullikson, and J. C. Davis, "X-ray interactions: photoabsorption, scattering, transmission, and reflection at $E = 50$–30000 eV, $Z = 1$–92," At. Data Nucl. Data Tables **54**, 181–342 (1993).

24. R. Soufli, S. L. Baker, J. C. Robinson, T. J. McCarville, M. J. Pivovaroff, S. P. Hau-Riege, and R. Bionta, "Morphology, microstructure, stress and damage properties of thin film coatings for the LCLS x-ray mirrors," Proc. SPIE **7361**, 73610U (2009).

25. http://henke.lbl.gov/optical_constants/.

26. G. E. Jellison, Jr., and F. A. Modine, "Parameterization of the optical functions of amorphous materials in the interband region," Appl. Phys. Lett. **69**, 371–373 (1996).

27. D. T. Pierce and W. E. Spicer, "Electronic structure of amorphous Si from photoemission and optical studies," Phys. Rev. B **5**, 3017–3029 (1972).

28. The data are available on request at the following e-mail address: larruquert@io.cfmac.csic.es.

29. J. Tauc, R. Grigorovici, and A. Vancu, "Optical properties and electronic structure of amorphous germanium," Phys. Status Solidi **15**, 627–637 (1966).

30. J. Tauc, "Optical properties and electronic structure of amorphous Ge and Si," Mat. Res. Bull. **3**, 37–46 (1968).

31. M. L. Theye, "Optical properties of a-Ge, a-Si and a-III-V compounds," in *Amorphous and Liquid Semiconductors*, Volume 1, J. Stuke and W. Brenig, eds. (Taylor & Francis, 1974). It contains part of the proceedings of the International Conference on Amorphous and Liquid Semiconductors held at Garmisch-Partenkirchen, Germany, in 1973.

32. O. Stenzel, *The Physics of Thin Film Optical Spectra: An Introduction* (Springer-Verlag, 2005), p. 214.

33. E. Shiles, T. Sasaki, M. Inokuti, and D. Y. Smith, "Self-consistency and sum-rule tests in the Kramers–Kronig analysis of optical data: applications to aluminium," Phys. Rev. B **22**, 1612–1628 (1980).

34. Downloaded from the following web of Physical Reference Data, Physics Laboratory at NIST: http://physics.nist.gov/PhysRefData/FFast/html/form.html.

35. M. Altarelli, D. L. Dexter, H. M. Nussenzveig, and D. Y. Smith, "Superconvergence and sum rules for the optical constants," Phys. Rev. B **6**, 4502–4509 (1972).

36. M. Altarelli and D. Y. Smith, "Superconvergence and sum rules for the optical constants: physical meaning, comparison with experiment, and generalization," Phys. Rev. B **9**, 1290–1298 (1974).

37. M. Fernández-Perea, J. I. Larruquert, J. A. Aznárez, J. A. Méndez, M. Vidal, E. Gullikson, A. Aquila, R. Soufli, and J. L. G. Fierro, "Optical constants of electron-beam evaporated boron films in the 6.8–900 eV photon energy range," J. Opt. Soc. Am. A **24**, 3800–3807 (2007).

38. M. Fernández-Perea, M. Vidal-Dasilva, J. I. Larruquert, J. A. Aznárez, J. A. Méndez, E. Gullikson, A. Aquila, and R. Soufli, "Optical constants of evaporation-deposited silicon monoxide films in the 7.1–800 eV photon energy range," J. Appl. Phys. **105**, 113505 (2009).